

Synthesis of a Novel Amphoteric Chelating Polymer Flocculant and its Performance in Cu^{2+} Removal

Lihua Liu, Jun Wu, Yulin Ling, Xin Li, Rongjin Zeng

Key Laboratory of Theoretical Chemistry and Molecular Simulation of Ministry of Education and Hunan Province, Hunan Province College Key Laboratory of QSAR/QSPR, School of Chemistry and Chemical Engineering, Hunan University of Science and Technology, Xiangtan, Hunan 411201, People's Republic of China

Correspondence to: L. Liu (E-mail: llh213@163.com)

ABSTRACT: A novel amphoteric chelating polymer flocculant (ACPF) was synthesized. The synthesis involved the copolymerization of dimethyldiallylammonium chloride and acrylamide to prepare poly(dimethyldiallylammonium chloride-*co*-acrylamide) [P(DMDAAC-*co*-AM)], Mannich reaction of P(DMDAAC-*co*-AM) with triethylenetetramine and formaldehyde to prepare P(DMDAAC-*co*-AM)-*graft*-TETA, and xanthogenation of P(DMDAAC-*co*-AM)-*graft*-TETA with CS_2 and NaOH. The removal performance of ACPF toward Cu^{2+} was investigated, and the ACPF structure was characterized. ACPF performance considerably improved at 121–187 mL/g intrinsic viscosity, 20.78–28.32 mol % cationic degree of P(DMDAAC-*co*-AM), and 22.11–28.44% sulphur content of ACPF. The Cu^{2+} removal rate was above 99% at a 1.98 : 1 molar ratio of $-\text{CSS}^-$ to Cu^{2+} . This rate was 5.86% higher than that using polyacrylamide-*graft*-triethylenetetramine-dithiocarbamate (PAM-*graft*-TETA-DTC). The zeta potential and sedimentation rate of flocs obtained from ACPF were higher and their volume was smaller than those from sodium triethylenetetramine-multidithiocarbamate and PAM-*graft*-TETA-DTC at the same sulphur dosage. This result indicates that the positive charges of ACPF polymeric chains effectively neutralize excess negative charges in flocs, which benefits the bridging of flocs with negative charges to promote their formation and growth. These positive charges can also cause the flocs to become larger and tighter, thereby improving flocculation and settling performance. © 2012 Wiley Periodicals, Inc. *J. Appl. Polym. Sci.* 000: 000–000, 2012

KEYWORDS: amphoteric chelating polymer flocculant; xanthation; chelation; flocculation; removal efficiency

Received 12 November 2010; accepted 27 March 2012; published online

DOI: 10.1002/app.37801

INTRODUCTION

The disposal of waste or process water containing heavy metal ions is a serious consideration in the chemical, metallurgical, mineral, petroleum, synfuel, cosmetics, and textile industries.^{1–4} Available technologies such as chemical precipitation,^{5,6} ferrite method,^{7,8} oxidation,^{9,10} ion exchange,¹¹ adsorption,^{12–14} membrane separation,¹⁵ and electrochemical method¹⁶ are used to remove heavy metal ions from water. However, these approaches have several disadvantages. For example, the removal efficiencies of traditional chemical precipitation methods such as alkaline deposition and sulfide precipitation are relatively low. The residual heavy metal concentration in the liquid phase is also often higher than the limit imposed by law. The operation of the ferrite method is complex and uncontrollable. Other methods show poor selectivity, complex operation, high cost, and suitability only for small-scale wastewater treatments.

Among the currently available chemical precipitation methods, chelating precipitation is a practical, highly efficient, and low-cost treatment method especially suitable for the treatment of large volumes of heavy metal wastewater.^{17,18} When using polymeric chelants as chelating agents, the negative charges of the polymeric chains can be neutralized by heavy metal ions, causing the polymer chains to twist and flocculate. Polymeric chains benefit the bridging among microflocs. The same heavy metal ions can also react with two or more chelating groups from different polymer chains to cause small flocs to gather and merge into larger ones. Therefore, some polymeric chelants possess favorable chelating abilities and excellent flocculating properties.^{19,20} These features can overcome the shortcomings of traditional precipitation methods such as small flocs, poor settling performance, and required high dosages to achieve better effects.²¹ Polymeric chelants have become a research hotspot in the treatment of heavy metal wastewater in recent years. For example, water-soluble starch xanthate can effectively remove Hg(II) and Cu(II) but not Cd(II) and

© 2012 Wiley Periodicals, Inc.

Ni(II).²² Cross-linked starch-*graft*-polyacrylamide-*co*-sodium xanthate (CSAX) is more effective than both cross-linked starch xanthate and cross-linked starch-*graft*-polyacrylamide in removing Cu²⁺ from wastewater; the removal rate of CSAX can reach >98%.¹⁹ Using polyethyleneimine-sodium xanthogenate for the treatment of wastewater from an electroplating factory results in removal rates of above 95% for Ni²⁺, Cu²⁺, and Cr⁶⁺ ions.²⁰ Phosphonomethylated-polyethyleneimine for metal separation by flocculation enhanced by Ca²⁺ can effectively remove various heavy metal ions such as Cu²⁺, Co²⁺, Zn²⁺, Ni²⁺, and Pb²⁺ from aqueous solutions. Under optimized conditions, the process is capable of scavenging Cu²⁺ ions to background levels.^{23,24} However, during chelation, steric hindrance and spatial mismatch always exist,²¹ resulting in the failure of some functional groups to chelate with heavy metal ions. Consequently, flocs with excess negative charges that hinder their formation and growth are created. The flocs formed are generally not compact and exhibit poor sedimentation performance. Thus, some flocculants are always needed in the treatment process.

To solve the above problems, this article introduced a certain amount of cationic structure units into polymer chains to synthesize a kind of amphoteric chelating polymer flocculant (ACPF). The synthetic conditions were investigated and the structure of the ACPF was characterized by Fourier-transform infrared (FTIR), nuclear magnetic resonance (NMR), ultraviolet (UV) spectroscopy, and elementary analyses. The removal performance of ACPF toward heavy metal ions was evaluated using simulated wastewater containing Cu²⁺. ACPF is found to be a new type of heavy metal treatment agent with a strong chelating ability and excellent flocculation performance.

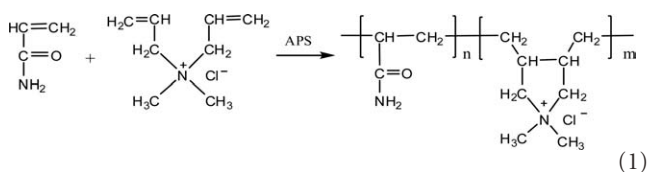
EXPERIMENTAL

Materials

Dimethyldiallylammonium chloride (DMDAAC; 60 wt % in water) was purchased from TCI, Tokyo Kasei Kogyo Co., Acrylamide (AM; Tianjin Damao Chemical Reagent Company, China) was analytical grade and recrystallized twice before use. Ammonium persulfate (APS; Zibo Xinglu Chemical Co., China), formaldehyde (37%, w/w; Jiangsu Taicang Jiantao Chemical Co., China), copper sulfate pentahydrate (Changsha Antai Fine Chemical Co., China), triethylenetetramine (TETA; 99.50%, w/w), carbon disulfide (99.0%, w/w), and sodium hydroxide (NaOH; Shantou Xilong Chemical Co., China) were all analytical grade. Deionized water was used in all experiments.

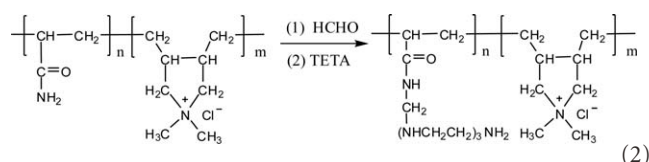
Preparation of ACPF

Preparation of Poly(dimethyldiallylammonium chloride-*co*-acrylamide). A series of poly(dimethyldiallylammonium chloride-*co*-acrylamide) [P(DMDAAC-*co*-AM)] samples with different cationic degrees (CDs) were prepared using DMDAAC, AM, and APS as raw materials. The reaction was as follows:



P(DMDAAC-*co*-AM) was prepared according to a DMDAAC to AM molar ratio of (0.05–0.45) : 1. The total mass of monomers (DMDAAC + AM) was 20 g. All proportions of DMDAAC and equimolar AM were dissolved in deionized water with mechanical stirring to prepare a certain solution with a 40% (w/w) concentration in a 250 mL three-necked flask. The mixture was deaerated with nitrogen for 30 min. Afterward, the polymerization reaction was initiated by the addition of APS with 0.8–1.2% monomer mass, and the temperature was maintained between 50 and 60°C. The remaining AM was used to prepare a 10% (w/w) solution using deionized water. The solution was slowly added to the reaction mixture to react for 1–5 h, after which a white or yellowish viscous liquid was obtained. This liquid was precipitated in anhydrous acetone three times, and the precipitates were dried to constant weight under vacuum at 60°C to obtain P(DMDAAC-*co*-AM) (Table I).

Preparation of Poly(dimethyldiallylammonium chloride-*co*-acrylamide)-*graft*-triethylenetetramine. To facilitate the easy introduction of xanthogenic acid radicals into the polymer chains, TETA was grafted onto the side chains of P(DMDAAC-*co*-AM) by the Mannich reaction of P(DMDAAC-*co*-AM) with TETA and formaldehyde to prepare poly(dimethyldiallylammonium chloride-*co*-acrylamide)-*graft*-triethylenetetramine [P(DMDAAC-*co*-AM)-*graft*-TETA]. The reaction was as follows:



P(DMDAAC-*co*-AM) (5 g) was dissolved in deionized water to prepare a 1–5% (w/w) solution. The pH was adjusted to within 10–10.5 using a diluted NaOH solution, and formaldehyde was added to react at 50°C for 40 min. A certain amount of TETA was added to react for another 3 h until a yellowish viscous solution was obtained. Afterward, the reaction mixture was precipitated in anhydrous acetone. The precipitates were washed with anhydrous acetone, dissolved in a little deionized water, and precipitated again. This step was repeated five times. The precipitates obtained were dried to constant weight in a vacuum oven at 50°C to obtain P(DMDAAC-*co*-AM)-*graft*-TETA.

Preparation of Poly(dimethyldiallylammonium chloride-*co*-acrylamide)-*graft*-triethylenetetramine-dithiocarbamate (ACPF). ACPF was prepared from P(DMDAAC-*co*-AM)-*graft*-TETA, NaOH, and CS₂. The reaction of the TETA moiety of P(DMDAAC-*co*-AM)-*graft*-TETA with CS₂ in the presence of NaOH is a nucleophilic addition reaction.²⁵ The negative charge density of the secondary nitrogen is higher than that of the primary nitrogen, and the secondary dithiocarbamate (DTC) is more stability than the primary DTC.²⁶ Consequently, CS₂

Table I. Raw Material Ratios, Polymerization Conditions, $[\eta]$, CD, and Yield of P(DMDAAC-co-AM)

Entry no.	n(DMDAAC): n(AM)	APS (mg·g ⁻¹ monomer)	Polymerization		P(DMDAAC-co-AM)		
			Temperature (°C)	Time (h)	$[\eta]$ (mL·g ⁻¹)	CD (mol %)	Yield (%)
1	0.05 : 1	160	50	2	497	4.71	98.9
2	0.05 : 1	180	50	1.5	213	4.65	93.4
3	0.05 : 1	200	50	1	167	4.58	82.6
4	0.05 : 1	220	55	1	143	4.51	84.7
5	0.10 : 1	160	50	3.5	403	8.99	98.5
6	0.10 : 1	180	50	3	329	8.82	97.8
7	0.10 : 1	200	50	2.5	236	8.37	93.5
8	0.10 : 1	220	50	2	187	8.16	87.7
9	0.10 : 1	240	50	1.5	125	8.23	86.2
10	0.10 : 1	200	50	1	83	8.02	76.7
11	0.15 : 1	160	55	4	400	12.11	98.4
12	0.15 : 1	180	55	3.5	337	11.94	96.4
13	0.15 : 1	200	55	3	232	12.01	95.3
14	0.15 : 1	220	55	2.5	183	11.85	92.4
15	0.15 : 1	220	55	2	137	11.24	87.6
16	0.15 : 1	240	55	2	133	11.78	88.9
17	0.15 : 1	240	55	1	79	11.65	78.5
18	0.20 : 1	160	55	4.5	392	16.58	98.4
19	0.20 : 1	180	55	3.5	295	16.43	96.4
20	0.20 : 1	200	55	3	202	16.51	94.3
21	0.20 : 1	220	55	2.5	182	16.29	91.4
22	0.20 : 1	230	55	2	131	16.35	88.7
23	0.20 : 1	240	55	1.5	91	16.10	81.8
24	0.30 : 1	160	55	4.5	410	23.85	98.3
25	0.30 : 1	180	55	3.5	325	23.99	96.6
26	0.30 : 1	200	55	3	243	24.51	92.8
27	0.30 : 1	220	55	2.5	179	23.09	87.2
28	0.30 : 1	240	55	2	125	24.37	82.4
29	0.30 : 1	230	60	1	120	20.78	83.5
30	0.30 : 1	240	55	1	75	23.72	75.7
31	0.40 : 1	160	55	4.5	398	28.51	97.6
32	0.40 : 1	180	55	4	331	28.34	95.9
33	0.40 : 1	200	55	3	233	27.98	91.8
34	0.40 : 1	220	55	2.5	177	28.12	87.1
35	0.40 : 1	240	55	2	131	28.03	81.4
36	0.40 : 1	200	55	1	84	27.91	72.4
37	0.45 : 1	160	55	5	404	29.72	98.1
38	0.45 : 1	180	55	4	335	28.95	96.4
39	0.45 : 1	200	55	3	235	29.04	94.4
40	0.45 : 1	220	55	2	185	29.36	92.1
41	0.45 : 1	240	60	2	134	30.13	87.7
42	0.45 : 1	220	60	1.5	128	28.32	85.4
43	0.45 : 1	230	60	2	119	27.43	86.5
44	0.45 : 1	240	60	1	67	28.73	74.9

Table III. The Effect of the Molar Ratio of AM Units and HCHO to TETA on the AR of P(DMDAAC-*co*-AM)-*graft*-TETA

Entry no.	Molar ratio (AM unit/HCHO/TETA)	AR (mol %)	Yield ^a (%)	Entry no.	Molar ratio (AM unit/HCHO/TETA)	AR (mol %)	Yield ^a (%)
1	1.0 : 0.5 : 0.5	28.6	59.8	7	1.0 : 0.9 : 0.9	52.9	73.5
2	1.0 : 0.5 : 0.6	30.7	61.0	8	1.0 : 0.9 : 1.08	53.4	73.8
3	1.0 : 0.5 : 0.75	31.9	61.7	9	1.0 : 0.9 : 1.35	53.8	74.0
4	1.0 : 0.8 : 0.8	47.8	70.7	10	1.0 : 1.0 : 1.0	54.2	74.2
5	1.0 : 0.8 : 0.96	50.9	72.4	11	1.0 : 1.0 : 1.2	55.3	74.9
6	1.0 : 0.8 : 1.2	51.1	72.5	12	1.0 : 1.0 : 1.5	56.5	75.5

^aBased on AM units, the theoretical yields of P(DMDAAC-*co*-AM)-*graft*-TETA are calculated according to all AM units grafted with TETA.

within the 4000–400 cm⁻¹ range. The NMR spectra were recorded with an AVANCE II superconductive nuclear magnetic resonance spectrometer (Bruker Co., Germany). The UV spectra of ACPF and the chelate of ACPF-Cu were determined by a Lambda 35 spectrophotometer (PerkinElmer Co., Shelton/Connecticut, USA) using deionized water as the solvent. The reference solutions for ACPF and ACPF-Cu testing were deionized water and a solution of 5 × 10⁻⁶ mol/L ACPF, respectively. The intrinsic viscosity ([η]) of P(DMDAAC-*co*-AM) was measured using an Ubbelohde viscometer (inner diameter of the capillary column φ = 0.55–0.65 mm; measuring temperature, 30°C; sample concentration, 0.5 g/L using 1.0 mol/L NaCl solution as solvent). The CD of P(DMDAAC-*co*-AM) was determined using the chloride ion-selective electrode method.²⁷ Elemental sulphur content was measured with a Vario EL III elementary analysis instrument (Elementar Co., Germany) at 950°C.

Determination of the AR of P(DMDAAC-*co*-AM)-*graft*-TETA

After 50 mL of deionized water was placed in a 250 mL conical flask, 4–5 drops of methyl red-bromocresol green mixed indicator were added. The solution was shaken and titrated with 0.1 mol/L hydrochloric acid standard solution until the green tint of the solution vanished. There was no need to record the volume of the titrant consumed. About 2–3 mmol AM units of P(DMDAAC-*co*-AM) were accurately weighed and added to the conical flask for dissolution (at this point, the color of the solution became green again). The solution obtained was again titrated with 0.1 mol/L hydrochloric acid standard solution until the green tint vanished. The solution became colorless or reddish, and the volume of hydrochloric acid consumed was recorded.

The AR of P(DMDAAC-*co*-AM)-*graft*-TETA was defined as the molar ratio of the AM units grafted with TETA to the total AM units of P(DMDAAC-*co*-AM)-*graft*-TETA. The AR of P(DMDAAC-*co*-AM)-*graft*-TETA was calculated as follows:

$$\text{mol\% AR} = \frac{c \cdot V}{n \cdot m - 158.24c \cdot V - 161.67n \cdot n_{\text{DMDAAC}}} \times 100 \quad (4)$$

where *c* and *V* are the concentration and consumption volume of the hydrochloric acid standard solution, respectively; *n* is the number of nitrogen atom on each side chain of P(DMDAAC-*co*-AM)-*graft*-TETA that can be titrated by hydrochloric acid (in this study, *n* = 4); *m* is the mass of the P(DMDAAC-*co*-AM)-*graft*-TETA sample, g; *n*_{DMDAAC} is the amount of DMDAAC units of P(DMDAAC-*co*-AM)-*graft*-TETA, mol, which can be

determined by the chloride ion-selective electrode method;²⁷ 158.24 is the formula weight difference between the AM unit grafted with TETA and the AM unit, equal to 229.32 minus 71.08; and 161.67 is the formula weight of a DMDAAC unit.

Measurement of Sedimentation Rate

Simulated wastewater containing 50 mg/L Cu²⁺ was poured into a 500 mL sedimentation graduated cylinder (the height of the part with the measurement scale is 25 cm). The flask was then placed on a S312-250 frequency conversion stirrer (Shanghai Shensheng Technology Co., China). The flocculation experiment was conducted under conditions similar to the above described flocculation test. Timekeeping was started as soon as stirring was stopped, and the descending height of the interface of the clear-turbid liquid was recorded at suitable intervals.

RESULTS AND DISCUSSION

ACPF is a yellowish or yellow hygroscopic powder, soluble in water, dilute salt solution, and dilute alkali solution. The structure of ACPF is complicated. Its [η] greatly depended on the amount of TETA grafted into AM units and the amount of -CSS⁻ in the side chains. Therefore, the relative molecular weight of ACPF cannot be suitably characterized by its intrinsic viscosity. In this paper, [η] and CD of P(DMDAAC-*co*-AM) were used to measure the size and amount of the positive charges of ACPF, respectively.

Synthesis of ACPF

Effect of Synthetic Conditions on the AR of P(DMDAAC-*co*-AM)-*graft*-TETA. Similar to polyacrylamide (PAM), the Mannich reaction takes place at the AM unit of P(DMDAAC-*co*-AM). Thus, the aminomethylation reaction conditions of PAM during the Mannich reaction can be used as Refs. 28–30, as confirmed by this experiments. Table III shows the effect of the molar ratio of AM units and HCHO to TETA on the AR of P(DMDAAC-*co*-AM)-*graft*-TETA. The [η] and CD of P(DMDAAC-*co*-AM) were 125 dL/g and 24.37 mol %, respectively. The pH was adjusted to 10.5, the temperature was 50°C, the methylation reaction time was 40 min, and the aminomethylation reaction time was 3 h.

At the same molar ratios of AM units to HCHO, the AR of P(DMDAAC-*co*-AM)-*graft*-TETA increases with increased molar ratio of TETA to HCHO. At the same molar ratio of HCHO to TETA (for example, nos. 1, 4, 7, and 10), AR increases with increased molar ratio of HCHO to AM units. The solubility of

Table IV. Effect of the $[\eta]$ of P(DMDAAC-*co*-AM) on the AR of P(DMDAAC-*co*-AM)-*graft*-TETA

Sample ^a	AR (mol %)	Yield ^b (%)	Sample ^a	AR (mol %)	Yield ^b (%)	Sample ^a	AR (mol %)	Yield ^b (%)
Entry 11	39.44	62.4	Entry 24	40.57	66.4	Entry 37	42.31	69.3
Entry 12	42.13	63.5	Entry 25	43.13	67.9	Entry 38	45.73	70.9
Entry 13	46.89	63.7	Entry 26	47.25	70.4	Entry 39	49.16	72.8
Entry 16	52.31	69.9	Entry 28	53.55	73.9	Entry 42	54.42	75.4
Entry 17	54.95	71.6	Entry 30	54.27	74.1	Entry 44	56.83	76.8

^aThe samples are listed in Table I and their numbers are in accordance with those in Table I, ^bBased on AM units, the theoretical yields of P(DMDAAC-*co*-AM)-*graft*-TETA are calculated according to all AM units grafted with TETA.

P(DMDAAC-*co*-AM)-*graft*-TETA in water also improves with increased molar ratio of TETA to HCHO. When the molar ratio of HCHO to AM units is 1.0 : 1.0, the solubility of P(DMDAAC-*co*-AM)-*graft*-TETA in water is relatively poor. This solubility improves only when the molar ratio of TETA to HCHO is 1.5 : 1.0. In the process of aminomethylation, AM units first react with HCHO to form hydroxymethylated P(DMDAAC-*co*-AM), then reacts with TETA to produce P(DMDAAC-*co*-AM)-*graft*-TETA. The methylol of hydroxymethylated P(DMDAAC-*co*-AM) easily reacts with another methylol to form an ether cross-link structure, or reacts with AM to form an intermolecular or intramolecular methylene cross-link structure.³⁰ Increased molar ratios of TETA to HCHO can reduce the amounts of free HCHO and residual hydroxymethylated P(DMDAAC-*co*-AM), thereby decreasing the cross-linking reaction they produce³¹ and increasing the stability as well as solubility of P(DMDAAC-*co*-AM)-*graft*-TETA. However, excessive TETA result in the decreased conversion rate of aminomethylation.³¹ Therefore, in terms of stability, solubility, and conversion rate, the optimum molar ratio of AM unit and HCHO to TETA is 1.0 : 0.9 : 1.08.

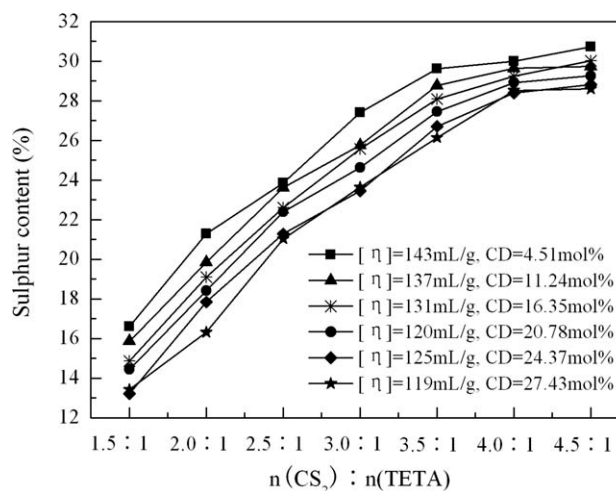
To investigate effect of the $[\eta]$ of P(DMDAAC-*co*-AM) on the AR of P(DMDAAC-*co*-AM)-*graft*-TETA, three groups of P(DMDAAC-*co*-AM) were used as experimental samples. For each group, the CDs of P(DMDAAC-*co*-AM) were close, but the $[\eta]$ values were different. The molar ratios of AM units and HCHO to TETA were all 1.0 : 0.9 : 1.08, and the procedures and other conditions were kept as described in the section Preparation of P(DMDAAC-*co*-AM)-*graft*-TETA. The results are shown in Table IV.

The AR of P(DMDAAC-*co*-AM)-*graft*-TETA increases with decreased $[\eta]$ of P(DMDAAC-*co*-AM) when the CD values are close. However, the change in AR is not obvious with increased CD when the $[\eta]$ values of P(DMDAAC-*co*-AM) are close. This result can be attributed to the increased crimp degree and neighboring group effect of macromolecular chains with increased $[\eta]$ of P(DMDAAC-*co*-AM), which hinders the reaction of P(DMDAAC-*co*-AM) with HCHO and TETA.²⁸

Effect of the Molar Ratio of CS₂ to TETA on the Sulphur Content of ACPF. Using P(DMDAAC-*co*-AM) with close $[\eta]$ values and different CD values as raw materials, the molar ratio of AM units and HCHO to TETA was set to 1 : 0.9 : 1.08. The effect of the molar ratio of CS₂ to TETA on the sulphur content of ACPF is shown in Figure 1.

When the $[\eta]$ and CD of P(DMDAAC-*co*-AM) remain unchanged, the sulphur content of ACPF rapidly increases as the CS₂ to TETA molar ratio increases before 3.5 : 1, after which the increase proceeds slowly. When the $[\eta]$ values of P(DMDAAC-*co*-AM) are close and the CS₂ to TETA molar ratio is the same, the sulphur content of ACPF decreases as the CD of P(DMDAAC-*co*-AM) increases. This is because with increasing CS₂ to TETA molar ratio, the equilibrium of eq. (3) gradually moves to the right, leading to increased sulphur content. When the molar ratio of CS₂ to TETA exceeds 3.5 : 1, the unreacted active groups of —NH— or —NH₂ in the molecular chain decrease, and the likelihood of xanthation decreases and —CSS[−] groups are difficult to introduce, resulting in a slow increase in sulphur content. Because the amount of AM units that can react with TETA and HCHO during the Mannich reaction decreases with increasing CD of P(DMDAAC-*co*-AM), the amount of grafted TETA decrease, leading to decreased sulphur content in ACPF at close $[\eta]$ values of P(DMDAAC-*co*-AM) and the same CS₂ to TETA molar ratios.

Effect of the $[\eta]$ of P(DMDAAC-*co*-AM) on the Sulphur Content of ACPF. The ACPFs were prepared from a series of P(DMDAAC-*co*-AM) samples with similar CDs but different $[\eta]$ synthesized according to five different molar ratios of DMDAAC to AM to understand the effect of the $[\eta]$ of P(DMDAAC-*co*-

**Figure 1.** Effect of the molar ratio of CS₂ to TETA on the ACPF sulphur content.

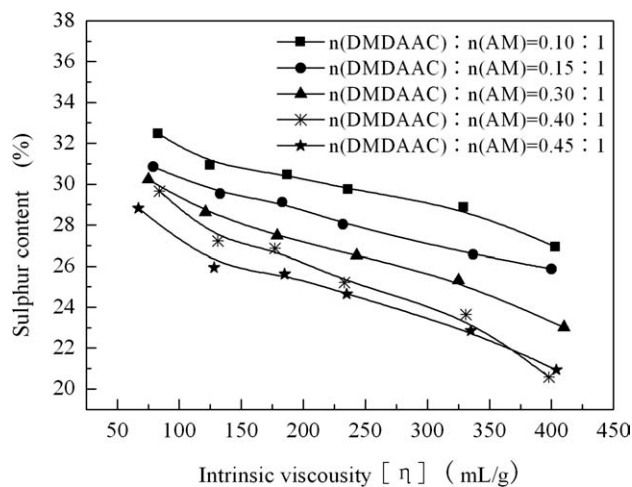


Figure 2. Effect of the $[\eta]$ of P(DMDAAC-*co*-AM) on the ACPF sulphur content.

AM) on the sulphur content of ACPF. The molar ratio of AM units, HCHO, TETA, and NaOH to CS₂ was 1 : 0.9 : 1.08 : 3.78 : 3.15. The results are shown in Figure 2.

For each group of P(DMDAAC-*co*-AM) prepared with the same molar ratio of DMDAAC to AM, the sulphur content of ACPF decreases with increased $[\eta]$ of P(DMDAAC-*co*-AM). When the $[\eta]$ values of P(DMDAAC-*co*-AM) are close, the sulphur content of ACPF also decreases with increased molar ratio of DMDAAC to AM. The sulphur content of ACPF depends on the amount of TETA moiety in P(DMDAAC-*co*-AM)-*graft*-TETA at the same molar ratios and synthetic conditions. The

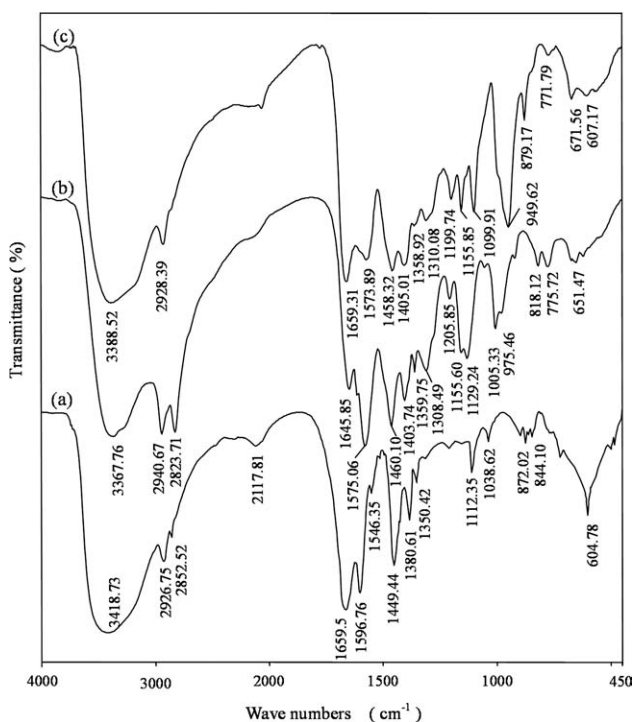


Figure 3. IR spectra of P(DMDAAC-*co*-AM) (a), P(DMDAAC-*co*-AM)-*graft*-TETA (b), and ACPF (c).

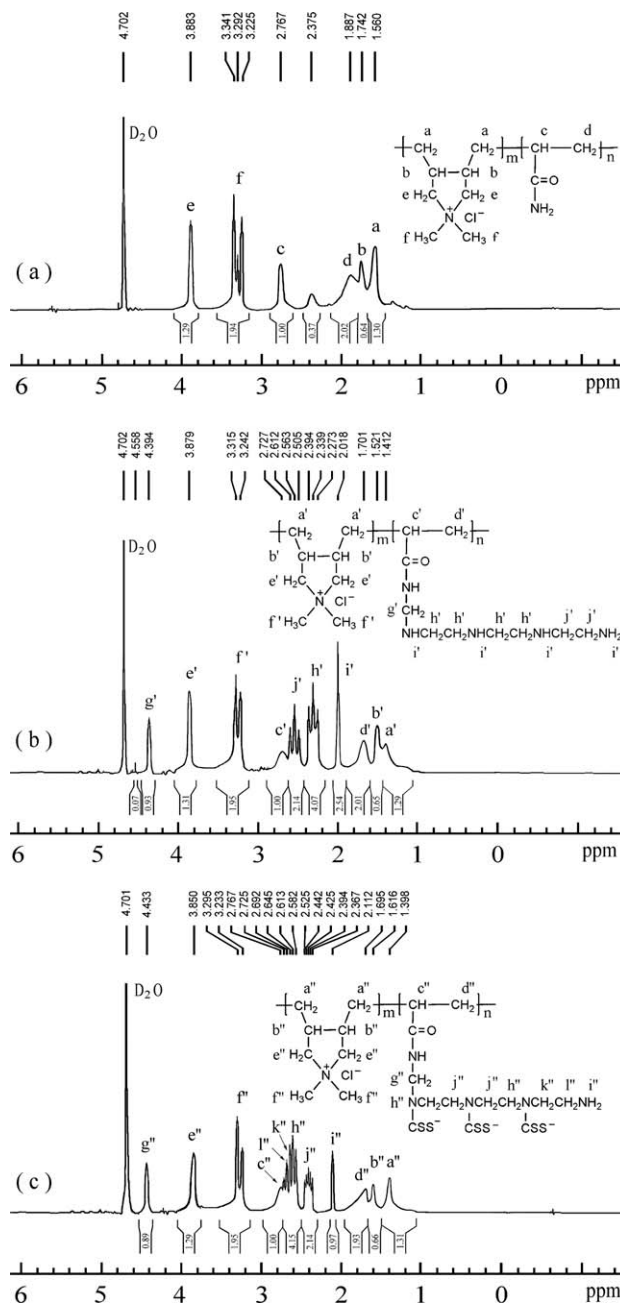


Figure 4. ¹H-NMR spectra of P(DMDAAC-*co*-AM) (a), P(DMDAAC-*co*-AM)-*graft*-TETA (b), and ACPF (c).

AR of P(DMDAAC-*co*-AM)-*graft*-TETA decreases with increased $[\eta]$ of P(DMDAAC-*co*-AM) (Table IV). The amount of AM moiety of P(DMDAAC-*co*-AM) decreases with increased molar ratio of DMDAAC to AM, leading to a decreased amount of TETA grafted. All these decreased amounts of —NH₂ and —NH— can cause xanthogenation, resulting in the decreased sulphur content of ACPF.

Characterization of the ACPF Structure

The IR, ¹H-NMR, and ¹³C-NMR spectra of P(DMDAAC-*co*-AM) ($[\eta]$ = 125 mL/g, CD = 24.37 mol %), P(DMDAAC-*co*-AM)-*graft*-TETA, and ACPF with 26.21% sulphur content

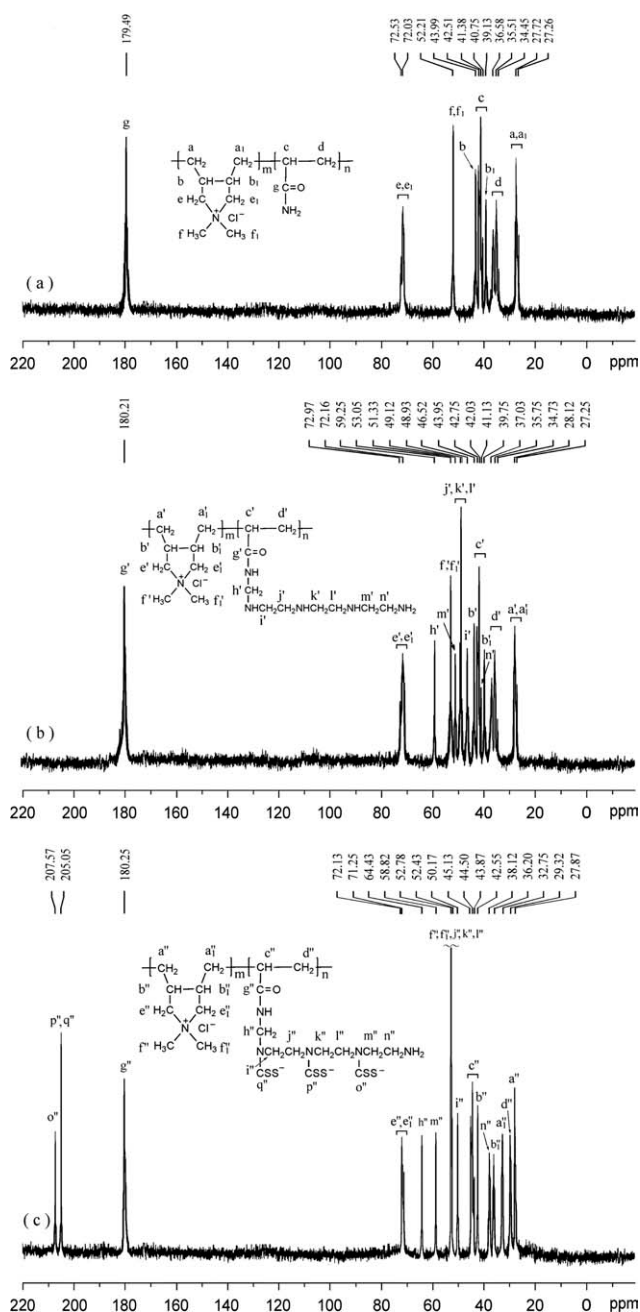


Figure 5. ^{13}C -NMR spectra of P(DMDAAC-*co*-AM) (a), P(DMDAAC-*co*-AM)-*graft*-TETA (b), and ACPF (c).

prepared from the P(DMDAAC-*co*-AM) above are presented in Figures 3–5, respectively.

In Figure 3(a), the broad absorption band observed at 3418.73 cm^{-1} is due to the stretching vibration of the N—H group of the AM unit and the O—H group of water absorbed from air during pellet-making due to the strong hygroscopicity of P(DMDAAC-*co*-AM).³² The bands around 1659.52 and 1546.35 cm^{-1} are respectively assigned to the C=O stretching vibrations and N—H deformation vibrations of the —CONH₂ group.^{32–34} The weak peaks at 1112.35 and 1038.62 cm^{-1} are due to C—N stretching vibrations.³⁴ The peaks at 2926.75 and 2852.52 cm^{-1}

are due to the C—H asymmetric stretching vibrations of CH₃— and C—H symmetric stretching vibrations of —CH₂—, respectively. The corresponding deformation vibration peaks of C—H appear at 1380.61 and 1350.42 cm^{-1} .³⁴ The peak at 1596.76 cm^{-1} is assigned to the deformation vibration of the quaternary ammonium ion N⁺ of the DMDAAC unit, and the peak at 1449.44 cm^{-1} is the deformation vibration of the double methyl linking to the quaternary ammonium ion.³⁵ Comparing Figure 3(a) with (b), (b) shows that the absorption peaks at 1155.60 and 1129.24 cm^{-1} , assigned to C—N stretching vibrations, are strengthened. Rocking vibrations of the —CH₂— of grafted TETA are observed at 818.12 and 775.72 cm^{-1} .³⁵ The peaks at 1005.33 and 975.46 cm^{-1} can be assigned to the skeletal vibrations of C—C.³⁵ The other peaks are similar to those in Figure 3(a), with only a small shift in wave number. These findings indicate that TETA has been successfully grafted onto P(DMDAAC-*co*-AM) macromolecules. The grafting can be confirmed by the ^1H -NMR spectra (Figure 4). In Figure 4(a) (D₂O, ppm), the characteristic peaks at 1.560 and 1.742 are assigned to the —CH₂— and —CH< protons of the DMDAAC unit, respectively. The peaks at 1.887 and 2.767 are assigned to the —CH₂— and —CH< protons of the AM unit, respectively.³⁶ The peaks at 3.225 , 3.292 , and 3.341 are assigned to —N⁺(CH₃)₂,³³ and the peak at 3.883 is assigned to N⁺—CH₂—.³³ Compared with Figure 4(a), four kinds of different characteristic peaks are found in Figure 4(b). A sharp peak at 2.018 ppm can be assigned to the NH₂— or —NH— proton of grafted TETA. The peaks at 2.273 to 2.394 and 2.505 to 2.612 are due to the —CH₂— proton of N—CH₂CH₂—N. Finally, the sharp peak at 4.394 can be assigned to the —CH₂— proton of —C(O)—NH—CH₂—NH—. The grafting is further proven by the ^{13}C -NMR spectra (Figure 5). In Figure 5(a), the peaks (ppm) at 179.49 , 40.75 – 42.51 , and 34.45 – 36.58 indicates the presence of AM units.³⁶ The peaks at 72.03 and 72.53 can be assigned to the carbon atom of N⁺—CH₂— of the DMDAAC unit (*e*, *e*₁), the peak at 52.21 to the carbon atom of N⁺—CH₃ (*f*, *f*₁), the peaks at 43.99 and 39.13 to the carbon of —CH< (*b*, *b*₁), and the peaks at 27.26 and 27.72 to the carbon atom of —CH₂— of the main chain (*a*, *a*₁). Compared with Figure 5(a), several new peaks (ppm) are found in Figure 5(b). The peak at 59.25 can be assigned to the carbon of —CH₂— of C(O)—NH—CH₂—NH— (*h*'), and the peaks at 51.33 , 49.12 , 48.93 , 46.52 , and 41.13 can be assigned to the carbons of the TETA moiety. The other peaks are similar to those in Figure 5(a), except for a small chemical shift.³⁵ All this findings reveal the presence of the TETA moiety.

Compared with Figure 3(a,b), strong absorption peaks at 1099.91 and 949.62 cm^{-1} , which can be assigned to the stretching vibrations of the C=S and C—S groups of —CSS[−],^{37–39} respectively, appear in Figure 3(c). This result can be further confirmed by the ^{13}C -NMR spectrum of ACPF [Figure 5(c)] with the appearance of peaks at 205.05 and 207.57 ppm, which can be assigned to the carbon atom of —CSS[−].⁴⁰ In Figure 3(c), the peak at 1458.32 cm^{-1} is assigned to either the deformation vibrations of double methyls linking to the quaternary ammonium ion, or the stretching vibrations of the C—N group of N—CSS[−].^{37,39} The peak at 879.17 cm^{-1} can be assigned to the deformation vibration of —CSS[−].³⁹ Compared with Figure 4(b),

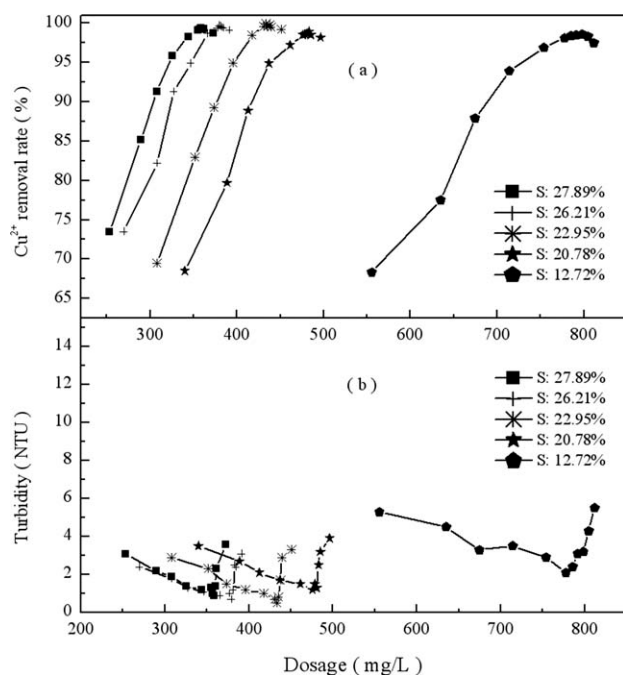


Figure 6. Effect of the ACPF dosage on the removal rate of Cu^{2+} (a) and residual turbidity of the supernatant (b).

the corresponding characteristic peaks in Figure 4(c) show shifts because of the $-\text{CSS}^-$ groups introduced into P(DMDAAC-*co*-AM)-*graft*-TETA macromolecules. The peak of the NH_2^- or $-\text{NH}-$ proton shifts to 2.112, whereas the peak of the $-\text{CH}_2-$ proton of $-\text{C}(\text{O})-\text{NH}-\text{CH}_2-\text{NH}$ shifts to 4.433. The peaks of $-\text{CH}_2-$ of $\text{N}-\text{CH}_2\text{CH}_2-\text{N}$ shift to 2.367–2.525 and 2.582–2.725.³⁵ Other characteristic peaks in Figure 4(c) are similar to those in Figure 4(b), except for a small chemical shift. Similarly, compared with Figure 5(b), the corresponding characteristic peaks in Figure 5(c) also show shifts due to the $-\text{CSS}^-$ groups introduced into P(DMDAAC-*co*-AM)-*graft*-TETA. Therefore, $-\text{CSS}^-$ has been successfully introduced into the molecular chain of ACPF.

Chelating Flocculation Effect

Effect of the ACPF Dosage on the Removal Efficiency of Cu^{2+} . Figure 6 shows the effect of the ACPF dosage with different sulphur contents on the removal efficiency of Cu^{2+} and residual turbidity of the supernatant. The ACPFs prepared from P(DMDAAC-*co*-AM) ($[\eta] = 125 \text{ mL/g}$, $\text{CD} = 24.37 \text{ mol } \%$) according to identical molar ratios of AM units and HCHO to TETA (1 : 0.9 : 1.08) and different molar ratios of CS_2 to TETA were used as the treatment agent. Simulated wastewater containing 50 mg/L Cu^{2+} was used as the test sample.

Figure 6(a) shows that for the same ACPF, the removal rate of Cu^{2+} initially rapidly increases with increased ACPF dosage, and then decreases when the dosage exceeds a certain amount. For different ACPFs, the dosage that achieves the same removal rate of Cu^{2+} increases with decreased sulphur content. The optimum removal rates of Cu^{2+} obtained are 98.6%, 98.9%, 99.9%, 99.7%, and 99.4%, respectively. However, when the optimum dosages of ACPF were converted into the amounts of

$-\text{CSS}^-$ according to sulphur content (the molar ratios of $-\text{CSS}^-$ to Cu^{2+} were 2.01 : 1, 1.99 : 1, 1.97 : 1, 1.97 : 1, and 1.98 : 1, respectively), the optimum molar ratios of $-\text{CSS}^-$ to Cu^{2+} are all surprisingly close to 2 : 1. This result means that two $-\text{CSS}^-$ groups chelate one Cu^{2+} ion. Based on the removal rates, the preferred sulphur contents of ACPF are 22.95% and 26.21%.

As shown in Figure 6(b), the corresponding residual turbidities of the supernatant are all close to 1 NTU near the optimum dosage. When the dosage exceeds the optimum amount, turbidity increases. Cu^{2+} ions possessing a d^9 electron structure tend to generate coordination compounds with coordination numbers of 4 or 6, whereas $-\text{CSS}^-$ is a kind of bidentate ligand.^{38,41} Therefore, Cu^{2+} can combine with two or three $-\text{CSS}^-$ groups to form a chelate. From the above molar ratio, ACPF combines with Cu^{2+} according to a 2 : 1 molar ratio of $-\text{CSS}^-$ to Cu^{2+} to form chelates with a coordination number of 4. The two $-\text{CSS}^-$ groups chelated with the same Cu^{2+} can come from the same or different side chains of the same backbones, or from different side chains of different backbones, as shown in Figure 7.

The steric positions of the two chelating groups need to match each other to form chelates. Therefore, the $-\text{CSS}^-$ groups on the side chains need to be of a certain amount and suitable distribution. When the amount of $-\text{CSS}^-$ groups is less than the optimum level, for example, when there is only one $-\text{CSS}^-$ group on each side chain, the groups need to cooperate with other $-\text{CSS}^-$ groups from the other side chains to combine with a Cu^{2+} ion. The two groups should also distribute at a suitable position; otherwise, the steric hindrance is large and the removal rate of Cu^{2+} is low. When there is more than one $-\text{CSS}^-$ group on the same side chain, the generation of chelates in the same side chain easily occurs when the groups are adjacent to each other; otherwise, chelation proceeds with difficulty. Some $-\text{CSS}^-$ groups that have matched to form chelates can still hinder the chelation of other $-\text{CSS}^-$ groups with Cu^{2+} . For example, the $-\text{CSS}^-$ group on the β' position (Figure 7) is difficult to chelate with Cu^{2+} to produce flocs with excess negative charges. This situation hinders the generation and growth of flocs. The positive charges of ACPF can effectively neutralize the excess negative charges, which is beneficial for promoting the generation and growth of flocs.

Effect of the ACPF Sulphur Content on the Removal Efficiency of Cu^{2+} . Using simulated wastewater containing 50 mg/L Cu^{2+} as a test sample, ACPF synthesized from P(DMDAAC-*co*-AM) with similar $[\eta]$ and different CD values, as well as PAM-*graft*-TETA-DTCs from PAM with $[\eta] = 113 \text{ mL/g}$ (Table II) as reagents, the dosage of ACPF or PAM-*graft*-TETA-DTC was added according to a 1.98 : 1 molar ratio of $-\text{CSS}^-$ to Cu^{2+} . The results of the effects of the ACPF sulphur content or PAM-*graft*-TETA-DTC on the removal efficiency of Cu^{2+} are shown in Figure 8.

For the ACPFs prepared from P(DMDAAC-*co*-AM) with the same $[\eta]$ and CD, the removal rate of Cu^{2+} initially increases with increased ACPF sulphur content, and then reaches a higher value when the sulphur content of ACPF is in the range of

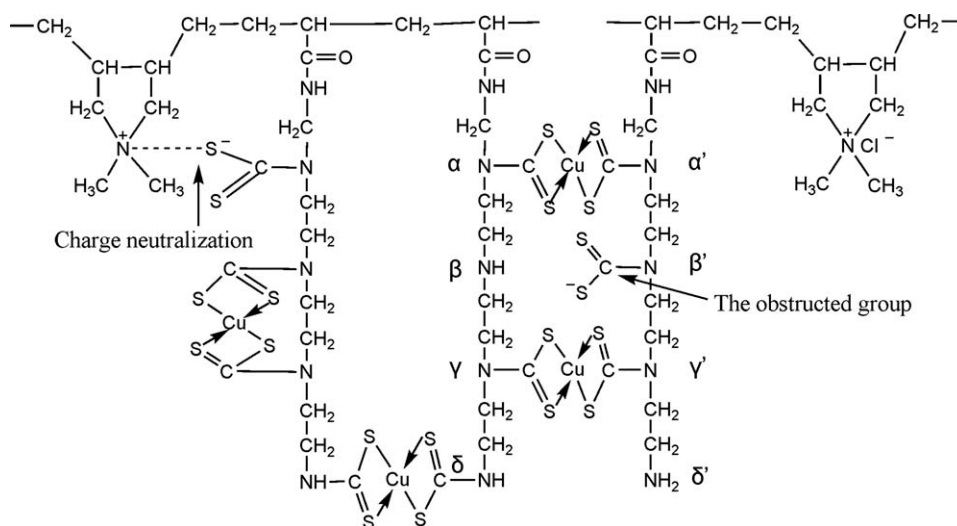


Figure 7. Representation of possible mechanism of chelation-flocculation.

22.11–28.44%. The removal rate of Cu^{2+} decreases as the sulphur content sequentially increases. When there are fewer $-\text{CSS}^-$ groups on the side chains of ACPF (Figure 7), chelation proceeds with difficulty. When the sulphur content, specifically, the number of $-\text{CSS}^-$ groups on the side chains increases, especially when the sulphur content reaches 22.11–28.44%, two or three $-\text{CSS}^-$ groups occur on each side chain, and their distribution on the chain is beneficial for chelate formation, thus the removal rate is high. When the sulphur content is above 28.44%, there are always more than three $-\text{CSS}^-$ groups on each side chain, leading to an increased number of $-\text{CSS}^-$ groups failing to chelate with Cu^{2+} due to steric hindrance and spatial mismatch. This phenomenon causes the excess negative charges on the flocs to increase, leading to decreased Cu^{2+} removal rate.

Figure 8 shows that the removal rate of Cu^{2+} is evidently influenced by the CD of P(DMDAAC-co-AM). When the CD is below 27.43 mol %, the removal rate of Cu^{2+} increases with increased CD of P(DMDAAC-co-AM). In contrast, the removal rate decreases when the CD reaches 30.13 mol %. When the CDs of P(DMDAAC-co-AM) are 20.78, 24.37, and 27.43 mol %, and the corresponding sulphur contents of ACPF are within the ranges of 22.29–29.35%, 22.45–28.21%, and 22.53–28.44%, the removal rates of Cu^{2+} are all above 99%, and the residual concentrations of Cu^{2+} are lower than the 0.5 mg/L limit set by the National Integrated Wastewater Discharge Standards of China. When PAM-graft-TETA-DTC is used as a chelating agent, the removal rate reaches the optimum value of 93.14% at a sulphur content of 27.85%, which is at least 5.86% lower than that using ACPF. The residual Cu^{2+} is 3.43 mg/L, much higher than the limit of 0.5 mg/L. This phenomenon may be due to the existence of steric hindrance and spatial mismatches in the chelating process, resulting in the constant presence of excess negative charges in the flocs, which hinder their generation and growth. However, the positive charges of the ACPF chains can effectively neutralize the excess negative charges to promote the formation and growth of flocs, thereby increasing the removal rate of

Cu^{2+} . The decrease in the removal rate of Cu^{2+} at a CD of 30.13 mol % may be due to the steric resistance of chelation, which increases with increased amount of DMDAAC units.

To prove the above viewpoints, the zeta potential changes of flocs using ACPF (sulphur content = 26.21%) and two control chelating agents, TETAMDT (sulphur content = 41.06%) and PAM-graft-TETA-DTC (sulphur content = 27.85%), were determined. The Cu^{2+} concentration of the simulated wastewater sample was 10 mg/L. The results are shown in Figure 9.

For ACPF, when the dosage of sulphur is less than 19.86 mg/L (the molar ratio of $-\text{CSS}^-$ to Cu^{2+} is below 1.97 : 1), the zeta potential of microflocs shows no significant change with increased sulphur dosage. However, at a sulphur dosage above 19.86 mg/L, the zeta potential decreases with increased dosage. Similar trends are found using TETAMDT or PAM-graft-TETA-

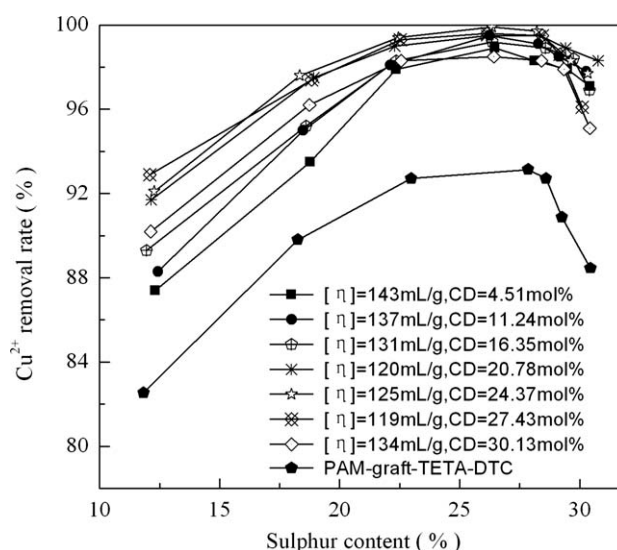


Figure 8. Effect of the sulphur content of ACPF or PAM-graft-TETA-DTC on the removal rate of Cu^{2+} .

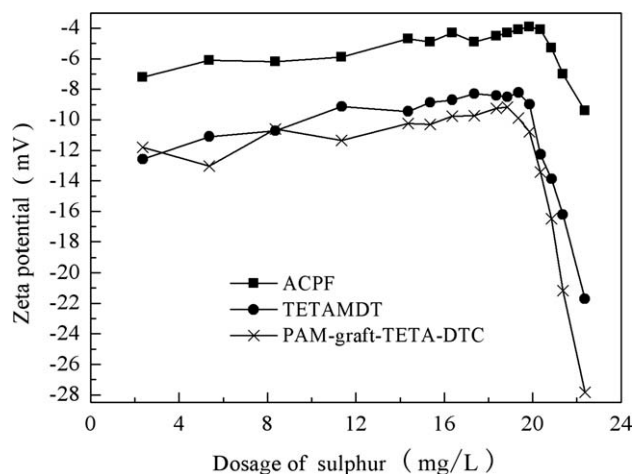


Figure 9. Effect of the dosage on the zeta potential of microflocs.

DTC as reagents. For TETAMDT, when the sulphur dosage is less than 19.36 mg/L (the molar ratio of $-\text{CSS}^-$ to Cu^{2+} is 1.92 : 1), there is little change in the zeta potential of the microflocs with increased sulphur dosage. The change further decreases with increased dosage when the sulphur dosage exceeds 19.36 mg/L. For PAM-graft-TETA-DTC, when the sulphur dosage is less than 18.86 mg/L (the molar ratio of $-\text{CSS}^-$ to Cu^{2+} is 1.87 : 1), there is little change in the zeta potential of the microflocs with increased sulphur dosage. The change further decreases with increased dosage when the sulphur dosage exceeds 18.86 mg/L. At equal sulphur dosages, the zeta potential of microflocs treated with ACPF is higher than that of flocs treated with TETAMDT and PAM-graft-TETA-DTC. The decrement of zeta potential using ACPF is less than that using TETAMDT or PAM-graft-TETA-DTC when the treatment dosages exceed the corresponding optimum sulphur dosage. Because of the zeta potential determined being the potential of the shear plane of the dispersed particles,⁴² before adding ACPF, the simulated solution is a clear solution and there is no zeta potential change. On ACPF addition, a Cu^{2+} ion chelates with

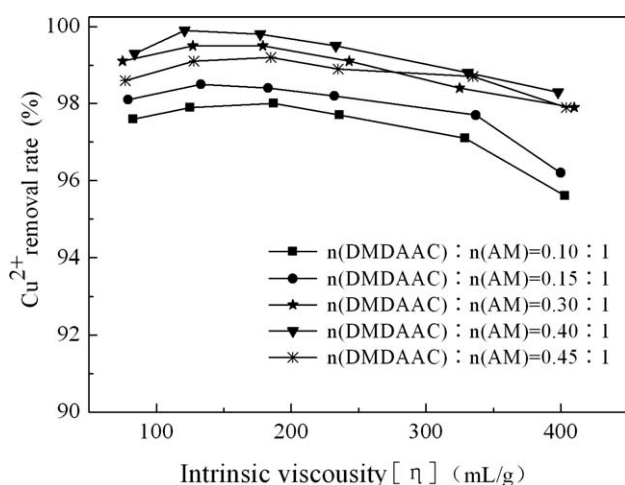


Figure 10. Effect of the $[\eta]$ of P(DMDAAC-co-AM) on the removal rate of Cu^{2+} .

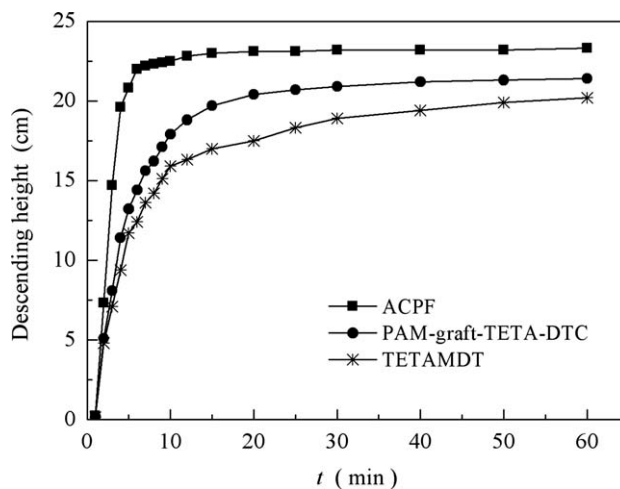


Figure 11. Descending height of the interface of clear-turbid liquid vs. the settling time.

two $-\text{CSS}^-$ groups from the same or different molecular chains to neutralize the negative charges of macromolecular chains to make them twist and form microflocs. The microflocs grow into larger flocs via adsorption or the combination of excess $-\text{CSS}^-$ groups from different microflocs by the same heavy metal ion in the mixing process. During this process, a change in the zeta potential occurs. When the dosage of $-\text{CSS}^-$ is less than the theoretical amounts (the molar ratio of $-\text{CSS}^-$ to Cu^{2+} is 2 : 1), the $-\text{CSS}^-$ group chelates with Cu^{2+} according to an almost definite stoichiometric ratio, regardless of the amount of Cu^{2+} in the solution. This phenomenon leads to microfloc charges close to each other. Thus, the change in the zeta potential is not evident with increased treatment dosage. Each molecule of ACPF, TETAMDT, and PAM-graft-TETA-DTC has more than one $-\text{CSS}^-$ group, so steric hindrance and spatial mismatches are inevitable. There are always some $-\text{CSS}^-$ groups failing to combine with Cu^{2+} , resulting in flocs with excess negative charges. ACPF chains feature quaternary ammonium ions such that the excess negative charges of flocs can be effectively neutralized. Therefore, the zeta potential of microflocs using ACPF is higher than those using TETAMDT and PAM-graft-TETA-DTC at the same sulphur dosage.

Effect of the $[\eta]$ of P(DMDAAC-co-AM) on the Removal Efficiency of Cu^{2+} . Figure 10 shows the effect of the $[\eta]$ of P(DMDAAC-co-AM) on the removal efficiency of Cu^{2+} . Using the ACPFs shown in Figure 2 as the reagent and simulated wastewater containing 50 mg/L Cu^{2+} as the test samples, the dosage of ACPF was added according to a molar ratio of $-\text{CSS}^-$ to Cu^{2+} of 1.98 : 1.

The removal rate of Cu^{2+} is high when the $[\eta]$ of P(DMDAAC-co-AM) is between 121 and 187 mL/g, and decreases with increased $[\eta]$ past a certain range. This result may be due to the minimal steric hindrance for combining Cu^{2+} and better flocculation performance when the $[\eta]$ of P(DMDAAC-co-AM) is between 121 and 187 mL/g. When $[\eta]$ is above 187 mL/g, the crimp degree of polymer chains increases with increased $[\eta]$ to increase the steric hindrance during the formation of chelates.

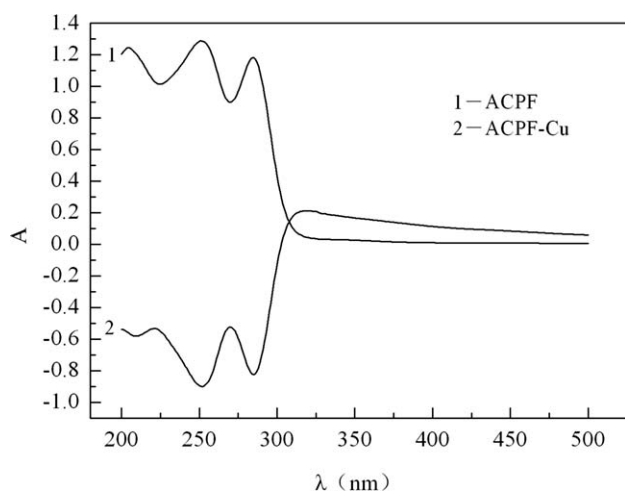


Figure 12. UV spectra of ACPF and ACPF-Cu.

Thus, the removal efficiency of Cu^{2+} is decreased. When $[\eta]$ is below 121 mL/g, the adsorption bridging action decreases although the steric hindrance of the polymer chains is low. Consequently, the removal efficiency of Cu^{2+} decreases.

Sedimentation Rate

Figure 11 shows the descending height of the interface of clear-turbid liquid using ACPF (sulphur content = 26.21%) prepared from P(DMDAAC-co-AM) ($[\eta]$ = 125 mL/g, CD = 24.37 mol %), TETAMDT (sulphur content = 41.06%), and PAM-graft-TETA-DTC (sulphur content = 27.85%) as reagents, as well as simulated wastewater containing 50 mg/L Cu^{2+} as the test sample. The dosages of ACPF, TETAMDT, and PAM-graft-TETA-DTC were added according to a molar ratio of $-\text{CSS}^-$ to Cu^{2+} of 1.98 : 1.

The order of the sedimentation rate of flocs is as follows: ACPF > PAM-graft-TETA-DTC > TETAMDT. The flocs completely settle within 10 min with ACPF, and within 25 min with PAM-graft-TETA-DTC, whereas the descending height of the interface of clear-turbid liquid with TETAMDT slowly increases after 30 min. At the settling time of 60 min, the height of the chelating precipitates is 1.77 cm with ACPF, 3.60 cm with PAM-graft-TETA-DTC, and 4.80 cm with TETAMDT. There still exist excess negative charges in the flocs formed due to steric hindrance or spatial mismatches regardless of the reagent used (ACPF, PAM-graft-TETA-DTC, or TETAMDT). A certain amount of positive charges on the ACPF chains can effectively neutralize the excess negative charges to promote the generation and growth of flocs. The polymer chains of ACPF also have strong sorption and bridging capabilities among microflocs. These attributes cause flocs from ACPF to become larger and tighter, leading to increased sedimentation rates and smaller volumes of chelating precipitates. There is no positive charge in PAM-graft-TETA-DTC or TETAMDT to facilitate the effective neutralization of the excess negative charges of flocs, resulting in increased repulsive force among microflocs. Therefore, the sedimentation rates of flocs are slower and the volumes of che-

lating precipitates are larger in flocs from PAM-graft-TETA-DTC or TETAMDT than in those from ACPF.

UV Spectra of ACPF and ACPF-Cu

To further investigate the formation of the chelating precipitates of ACPF-Cu, the UV spectra of ACPF and ACPF-Cu were obtained. The results are shown in Figure 12.

Maximum absorption peaks are observed at around 204, 251, and 285 nm in ACPF. The peak at 204 nm is due to the $n-\sigma^*$ transitions of a nonbonding electron localized on the sulphur atom of the $\text{S}-\text{C}=\text{S}$ group jumping to an antibonding σ orbital. The peak at 251 nm is the $\pi-\pi^*$ transition of the $\text{N}=\text{C}=\text{S}$ group, and the peak at 285 nm is the $\pi-\pi^*$ transition of the $\text{S}-\text{C}=\text{S}$ group.^{38,39,43} These findings indicate that there exist partial double bonds in the $\text{C}-\text{N}$ and $\text{C}-\text{S}$ bonds, further proving that there are $-\text{CSS}^-$ groups in the ACPF molecule.³⁹ Compared with ACPF, the maximum absorption of ACPF-Cu appearing at 319 nm shows an obvious red shift, indicating that the conjugated systems of the ligand molecule remarkably change and the chelate of ACPF-Cu is formed.

CONCLUSIONS

1. A novel ACPF was successfully prepared by the following processes: copolymerization of DMDAAC and AM to prepare P(DMDAAC-co-AM), the Mannich reaction of P(DMDAAC-co-AM) with TETA and formaldehyde to prepare P(DMDAAC-co-AM)-graft-TETA, as well as the xanthogenation reaction of P(DMDAAC-co-AM)-graft-TETA with CS_2 and NaOH to prepare ACPF.
2. The AR of P(DMDAAC-co-AM)-graft-TETA increased with increased molar ratio of TETA to HCHO, and decreased with increased $[\eta]$ of P(DMDAAC-co-AM). Under the same conditions, the sulphur content of ACPF increased with increased molar ratio of CS_2 to TETA, and decreased with increased CD and $[\eta]$ of P(DMDAAC-co-AM).
3. ACPF reacted with Cu^{2+} to form chelates of ACPF-Cu according to a 2 : 1 molar ratio of $-\text{CSS}^-$ to Cu^{2+} . When the $[\eta]$ and CD of P(DMDAAC-co-AM) were 121–187 mL/g and 20.78–28.32 mol %, respectively, and the ACPF sulphur content was between 22.11% and 28.44%, the performance of ACPF improved. The removal rate of Cu^{2+} was above 99% when the molar ratio of $-\text{CSS}^-$ to Cu^{2+} was up to 1.98 : 1. This rate was at least 5.86% higher than that using PAM-graft-TETA-DTC.
4. The measured results of zeta potential changes and the sedimentation rate of the flocs indicated that the positive charges of ACPF can effectively neutralize excess negative charges in the flocs to promote their generation and growth. Consequently, the flocs are enlarged and tightened, thereby improving their flocculation and settlement performance.

ACKNOWLEDGMENTS

This research was supported by the Nature Science Foundation of China (Grant No. 51078141) and Hunan Province Science and Technology Research Program (Grant No. 2010FJ3030).

REFERENCES

1. Jaber, M.; Miehe, J.; Delmotte, L. *Chem. Mater.* **2005**, *17*, 5275.
2. Daifullah, A. A. M. B.; Girgis, S.; Gad, H. M. H. *Mater. Lett.* **2003**, *57*, 1723.
3. Beatty, S. T.; Fischer, R. J.; Hagers, D. L.; Rosenberg, E. *Ind. Eng. Chem. Res.* **1999**, *28*, 4402.
4. Jiang, Y. J.; Gao, Q. M.; Yu, H. G.; Chen, Y. R.; Deng, F. *Micropor. Mesopor. Mater.* **2007**, *103*, 316.
5. Guillard, D.; Lewis, A. E. *Ind. Eng. Chem. Res.* **2002**, *41*, 3110.
6. Giannopoulou, I.; Panias, D. *Hydrometallurgy* **2008**, *90*, 137.
7. Xiang, L.; Yin, Y. P.; Jin, Y. J. *Mater. Sci.* **2002**, *37*, 349.
8. Timoshenko, T. G.; Pshinko, G. N.; Kornilovich, B. Y.; Bagrii, V. A.; Makovetskii, A. L. *J. Water Chem. Tech.* **2007**, *29*, 248.
9. Korshin, G. V.; Chang, H. S.; Frenkel, A. I.; Ferguson, J. F. *Environ. Sci. Technol.* **2007**, *41*, 2560.
10. Jiraroj, D.; Unob, F.; Hagège, A. *Water Res.* **2006**, *40*, 107.
11. Pan, B. C.; Zhang, Q. R.; Du, W.; Zhang, W. M.; Pan, B. J.; Zhang, Q. J.; Xu, Z. W.; Zhang, Q. X. *Water Res.* **2007**, *41*, 3103.
12. Barrera-Díaz, C.; Palomar-Pardavé, M.; Romero-Romo, M.; Ureña-Nuñez, F. *J. Polym. Res.* **2005**, *12*, 421.
13. Jing, X. S.; Liu, F. J.; Yang, X.; Ling, P. P.; Li, L. J.; Long, C.; Li, A. M. *J. Hazard. Mater.* **2009**, *167*, 589.
14. Gao, B. J.; Gao, Y. C.; Li, Y. B. *Chem. Eng. J.* **2010**, *158*, 542.
15. Sarkar, B.; DasGupta, S.; De, S. *Sep. Purif. Technol.* **2009**, *66*, 263.
16. Pruksathorn, K.; Damronglerd, S. *Korean J. Chem. Eng.* **2005**, *22*, 873.
17. Wang, W. F.; Huang, C. P. *China Water Wastewater* **2002**, *18*, 49 (in Chinese).
18. Zheng, H. L.; Chen, C. Y.; Yue, H. X.; Peng, D. J.; Li, Z. L. *Environ. Chem.* **2006**, *25*, 765 (in Chinese).
19. Chang, Q.; Hao, X. K.; Duan, L. L. *J. Hazard. Mater.* **2008**, *159*, 548.
20. Chang, Q.; Wang, G. *Chem. Eng. Sci.* **2007**, *62*, 4636.
21. Fu, F. L.; Chen, R. M.; Xiong, Y. *Sep. Purif. Technol.* **2006**, *52*, 388.
22. Chaudharis, A.; Tare, V. *J. Appl. Polym. Sci.* **1999**, *71*, 1325.
23. Navarro, R. R.; Tatsumi, K. *Sep. Sci. Technol.* **2002**, *37*, 203.
24. Navarro, R. R.; Wada, S.; Tatsumi, K. *Sep. Sci. Technol.* **2003**, *38*, 2327.
25. Jia, Y. Y.; Gao, B. Y.; Lu, L.; Wang, X. N.; Xu, X. M. *China Environ. Sci.* **2009**, *29*, 201 (in Chinese).
26. Sarin, V. K.; Kent, S. B. H.; Tam, J. P.; Merrifield, R. B. *Anal. Bio. Chem.* **1981**, *117*, 147.
27. Hou, S. J.; Ha, R. H. *Acta Polym. Sin.* **1995**, *3*, 349 (in Chinese).
28. Fong, D. J.; Kowalski, D. W. *J. Polym. Sci. Part A: Polym. Chem.* **1993**, *31*, 1625.
29. Schiller, A. M.; Suen, T. *J. Ind. Eng. Chem.* **1956**, *48*, 2132.
30. Cummings, T. F.; Shelton, J. R. *J. Org. Chem.* **1960**, *25*, 419.
31. Fang, D. B.; Guo, R. W.; Ha, R. H. *Acrylamide Polymers*; Chemical Industry Press: Beijing, **2006**.
32. Kutsevol, N.; Guenet, J.-M.; Melnyk, N.; Sarazin, D. *Macromol. Symp.* **2006**, *235*, 201.
33. Lu, S. J.; Lin, S. B.; Yao, K. D. *Starch/Stärke* **2004**, *56*, 138.
34. Tian, B. H.; Fan, B.; Peng, X. J.; Luan, Z. K. *J. Environ. Sci.* **2005**, *17*, 798.
35. Silverstein, R. M.; Webster, F. X.; Kiemle, D. J. *Spectrometric Identification of Organic Compounds*, 7th ed.; John Wiley & Sons, Inc.: Hoboken/New Jersey, **2005**.
36. Uv, C.; Cabesteny, J. *J. Appl. Polym. Sci.* **1991**, *42*, 2857.
37. Mthethwa, T.; Pullabhotla, V. S. R. R.; Mdluli, P. S.; Wesley-Smith, J. *Polyhedron* **2009**, *28*, 2977.
38. Fabretti, A. C.; Forghieri, F.; Giusti, A.; Preti, C.; Tosi, G. *Spectrochim. Acta.* **1984**, *40A*, 343.
39. Liao, Q. Q.; Wang, Z. Y.; Li, Y. J.; Xiang, B.; Cheng, R. M.; Zhang, Q. *J. Spectrosc. Spectr. Anal.* **2009**, *29*, 829 (in Chinese).
40. Pretsch, E.; Bühlmann, P.; Affolter, C. *Structure Determination of Organic Compounds Tables of Spectral Data*; Springer-Verlag: Berlin, **2000**.
41. Yang, Y. H.; Zuo, B. C.; Li, J. Y.; Chen, G. *Spectrochim. Acta Part A* **1996**, *52*, 1915.
42. Li, H.; Wei, S. Q.; Qing, C. L. *J. Colloid Interface Sci.* **2003**, *258*, 40.
43. Tombeux, J.; Van, P.; Eeckhaut, Z. *Spectrochim. Acta.* **1972**, *28*, 1943.